# A porous C/LiFePO$_4$/multiwalled carbon nanotubes cathode material for Lithium ion batteries

Guohui Qin [a,b], Qianqian Ma [a,b], Chengyang Wang [a,b,*]

[a] School of Chemical Engineering and Technology, Tianjin University, Tianjin 300072, China
[b] Synergetic Innovation Center of Chemical Science and Engineering, Tianjin 300072, China

## ARTICLE INFO

## ABSTRACT

Three dimensional (3D) porous C/LiFePO$_4$/MWCNTs was synthesized by a hybrid of *in situ* sol gel strategy and a facile electro-polymerization polyaniline technique and a simultaneous sintering progress. In combined with the 3D hierarchical pore topologies and high electronic conduction facilitating the kinetics of both electron transport and lithium ion diffusion within the particles, the optimized electrodes exhibit an ultrahigh rate capacity, stable charge/discharge cycle ability, and a comparative volume capacity. The synthesized LiFePO$_4$ composite offers a discharge capacity of 169.6mAhg$^{-1}$ (nearly to its the theoretical capability 170mAhg$^{-1}$) at the C/10 rate and delivers a good rate performance with a capacity of 141.9mAh g$^{-1}$ at a high rate of 20 C, and stable charge/discharge cycle ability (>95% capacity retention after 200 charge/discharge cycles).This non-organic facile synthesize avenue can be high desirable to prepare high-power electrode materials

## 1. Introduction

The olivine structure lithium iron phosphate LiFePO$_4$ has become one of the most attractive cathode electrode material candidates for Li-ion battery because of its physico-chemical characteristics, including a relatively high theoretical specific capacity of 170 mAh g$^{-1}$, a flat voltage profile (3.4 V vs. Li$^+$/Li), high safety, high thermal stability in the charged state, as well as environmental benignity, low cost and abundant material supply. However, its intrinsic demerits regarding the poor electronic conduction and sluggish ion diffusion remains a great challenge. Many approaches has been attempted to overcome the obstacles. The way to overcome the limitation of lithium-ion diffusion mainly depends on downsizing and controlling the morphology of the particle to decrease length of the lithium ion diffusion pathway inside the particle [1–5],while improvements in conductivity were commonly achieved by coating conductive layer [6–13].

Nevertheless, decreasing the size of the LiFePO$_4$ crystallites to nanosize level maintains shortening the lithium ion diffusion pathway, however, it usually introduce a low tap density, in turn, leads to a low volumetric capacity in practical application. Hence, Carbon coating based on a controlled morphology preparation method which gains the compromise of a high tap density and shorten the lithium ion diffusion pathway is more preferable to overcome

the disadvantages[14], an effective carbon coating with a homogeneous nano/sub-micro sized distribution is of great significance. Considering simple carbon coating or additive is exclude to obtain perfect rate performance, an electrode consisting of carbon-coated, submicro-sized crystalline LiFePO$_4$ with 3D porosity is appealing since it can provide fast electronic conduction in the solid phase and ion conduction at reasonable rates in both solid and liquid phases. This has been corroborated by recent work on porous carbon monoliths[15,16], showing a superior high-rate performance[29,30].In view of its facility in terms of synthesis and porous structure, the design is superior to insert subcmicro sized particles into a porous carbon matrix. Recently, CNTs providing 3D have receive a wide attention due to its most effective in reducing the resistance, and thus improving the electrochemical performance of the composite cathode[17–20].

The incorporation of LiFePO$_4$ with CNTs composites in order to achieve three dimensional porous LiFePO$_4$ architectures is a favorable approach because it achieves fast electronic and ion conduction, while keeping an acceptable tap density[21]. Zhou et al. combined the advantages of porous LiFePO$_4$ and carbon nanotubes (CNTs) and prepared LiFePO$_4$/CNTs cathode composites, presented a high-performance cathode material for high-energy density and high-power density lithium-ion batteries[22].However, the conductivity of the cathode material is left to be further improved and the other aspects such as modifying the dispersion of CNTs by choosing different precursors for LiFePO$_4$ should be carefully considered to make full use of the CNTs conductive network.

* Corresponding author. Tel.: +86 22 27890481; fax: +86 22 27890481.
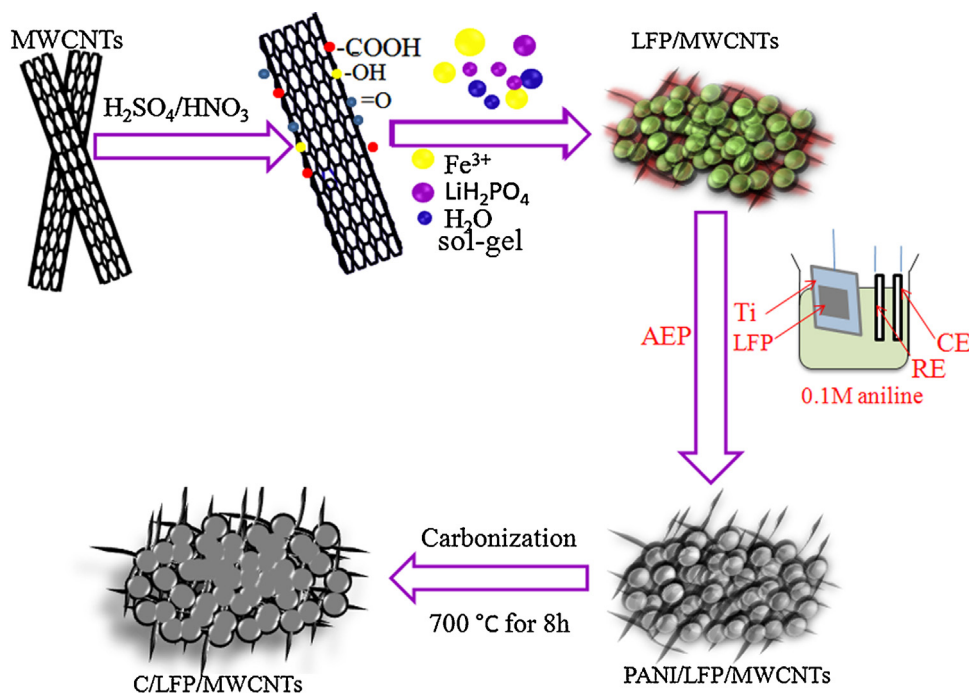E-mail address: cywang@tju.edu.cn (C. Wang).

**Fig. 1.** Schematic illustration of the synthesis procedure of C/LiFePO$_4$/MWCNTs submicro sized particles.

Herein, an alternative optimized sub-micro sized C/LiFePO$_4$/MWCNTs electrode structure design for high-power and high-energy lithium batteries by combining the advantages of porous submicro sized LiFePO$_4$ active particles and multiwalled carbon nanotubes (MWCNTs) networks has been developed. The precursor mixture (containing no carbon source) was prepared by a sol–gel method, which can mix components at molecular level. The synthesis process is illustrated in Fig. 1.This design interconnects the manifold benefits of MWCNTs, including high electronic conductivity, special tubular nanoscale morphology, corrosion resistance and high specific surface area to develop a highly-conductive tridimensional network which supply the porous LiFePO$_4$ structure, obtaining a high-performance composite cathode for high-energy and high-power lithium batteries. In order to further enhance the conductivity of the porous LiFePO$_4$/MWCNTs material, a uniform-thickness PANI coating was deposited on top of the interconnected LiFePO$_4$ primary particles using a facile electro-polymerization process after proceeded by a heat-treatment, which greatly enhances the conductivity of the sample by the overall carboncoating. The highly dispersed conductive networks could significantly facilitate the kinetics by ensuring sufficient electron supply, especially at high rates. The hierarchical porous C/LiFePO$_4$/MWCNTs composite performs improved conductivity, rate capabilities, a good cyclic behaviors, more important a comparative high tap density, which is promising as the high performance cathode material for lithium-ion batteries.

## 2. Experimental

### 2.1. Functionalization of MWCNTs

The MWCNTs (FloTube9000, purity ≥95 wt %, 20 nm in diameter, 10 μm in length) used in this work were provided by CNano Technology Ltd. These MWCNTs are about 10−20 nm in diameter and 10−30 μm in length with an approximate surface area of 500 m$^2$ g$^{-1}$.In order to increase the interfacing binding between the MWCNTs and LiFePO$_4$, MWCNTs has to be pre-treated by nitric acid for the surface functionalization [23].

Purification was firstly performed in order to remove the catalyst, MWCNTs was immerged in diluted sulfuric acid (50 wt %) at 120 °C for 5 h. Subsequently, MWCNTs were filtered by using glass frit, washed with distilled water, and dried at 120 °C for 12 h. Functionalized MWCNTs were prepared according to the previous work [24]. First, 0.01 g of purified MWCNTs were oxidized in 100 mL of HNO$_3$ and H$_2$SO$_4$ mixture (1:3 by volume) solution by refluxing at 70 °C for 8 h and sonicated for 4 h to perform a partial oxidation of the surface and the formation of oxidized groups such as C-OH-,-O-C=O or C=O (Fig. 2). Finally, the solution was filtered by vacuum filtration through a poly(tetrafluoroethylene)
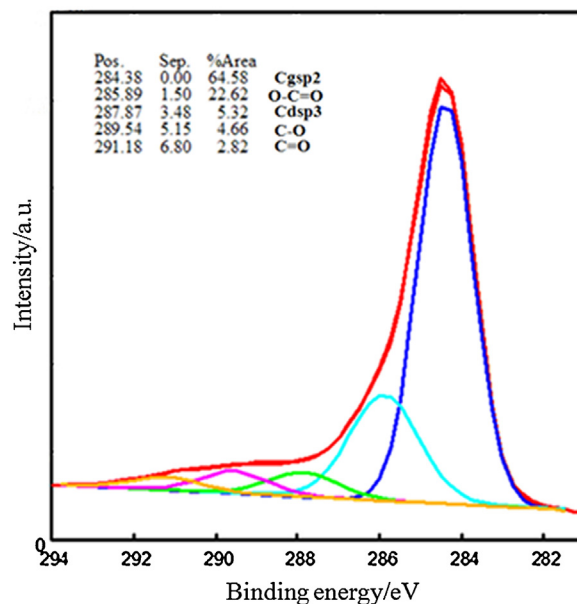


**Fig. 2.** Deconvoluted XPS spectra of functionalized MWCNTs.

(PTFE) filter (Millipore, 25 mm in diameter, 0.2 μm pores) and washed with distilled water. As depicted in Fig. 2, large amounts of oxygenated groups, hydroxyl, carbonyl and carboxyl groups were observed on the functionalized MWCNTs surface, indicting the strong chemical reactivity between LiFePO$_4$ and MWCNTs.

## 2.2. Preparation of C/LiFePO$_4$/MWCNTs

C/LiFePO$_4$/MWCNTs composite was prepared as cathode materials for lithium-ion batteries. Firstly, the porous LiFePO$_4$/MWCNTs composite with tridimensional networks were prepared by a facile *in situ* sol–gel method. The stoichiometric amounts of Fe(NO$_3$)$_3$, LiH$_2$PO$_4$ corresponding to 0.01 mol of LiFePO$_4$ were dissolved in 50 ml of distilled water under magnetic stirring. 0.158 g of pre-treated MWCNTs was dispersed in the mixture under the constant stirring. pre-treated MWCNTs was dispersed into the solution under ultrasonication, and then the mixture was treated with ultrasonic processing for half an hour. The obtained mixture was stirred by keeping it at 50 °C at least 12 h. After evaporating the water, the wet gel was developed, and then it was moved into a vacuum oven and heated at 120 °C for 12 h. The preparation of pure LiFeO$_4$ was the same as the above procedure except without the additive of MWCNTs.

In order to further improve the conductivity of the LiFePO$_4$/MWCNTs composite, a uniform-thickness PANI by using an anodic electro-polymerization (AEP) process was uniformly coated onto their surface to form a homogeneous PANI/LiFePO$_4$/MWCNTs composite. The in situ AEP process was conducted at a constant potential of 1 V for 600s in a three-electrode cell at room temperature. The LiFePO$_4$/MWCNTs composite were dispersed into ethanol and the solution was applied onto a titanium substrate to play a role of the working electrode. The PANI monomer (0.1 mol L$^{-1}$) in sulfuric acid (0.1 mol L$^{-1}$) was drafted as the electrolyte; and Hg/HgSO$_4$ and Pt mesh were designed as the reference and counter electrodes, respectively. After washing with distilled water and acetone several times, the collected PANI/LiFePO$_4$/MWCNTs composites were calcined at 700 °C for 8 h in a tubular furnace under a N$_2$ ambient to gain the interconnected carbon shell on the hierarchical porous of LiFePO$_4$/MWCNTs composite, restricting the in situ crystallite growth of LiFePO$_4$.

## 2.3. Characterizations

The X-ray diffraction (XRD) patterns of LiFePO$_4$ samples were obtained using a PANalytical X-pert diffractometer (PANalytical, Netherlands) with a Cu Kα radiation operated at 40 kV and 30 mA. Raman spectrum was measured by a Renishaw in ViaRaman microscope at room temperature with the 532 nm line of an Ar ion laser as an excitation source. X-ray photoelectron spectroscopy (XPS, VGMicro Tech) was used to measure the oxygen content in the functionalized MWCNTs. Morphology and structure of the samples were analyzed viafield-emission scanning electron microscopy (FE-SEM, S4800, Thermo Fisher) and high resolution transmission electron microscopy (HR-TEM, Tecnai G2F20, Philips).

The electrochemical performance of the LiFePO$_4$ samples were tested using a CR2025-type coin cell. To prepare the working electrodes, the active material powder, carbon black and poly(vinylidene fluoride) binder were mixed at a weight ratio of 80:10:10 in N-methyl-2-pyrrolidone solvent. The mixed viscous slurry was coated onto Al foil and dried at 120 °C under vacuum for 12 h. The obtained film was cut into circular discs with area of ~1.5 cm$^2$, and the discs were pressed at a pressure of 10 MPa to act as the working electrodes. The positive electrodes with approximately 2.3 mg of the active materials with a uniform thickness were assembled in coin cells with a lithium metal foil as the negative electrode, a Celgard 2400 film as the separator, and 1.0 M LiPF$_6$
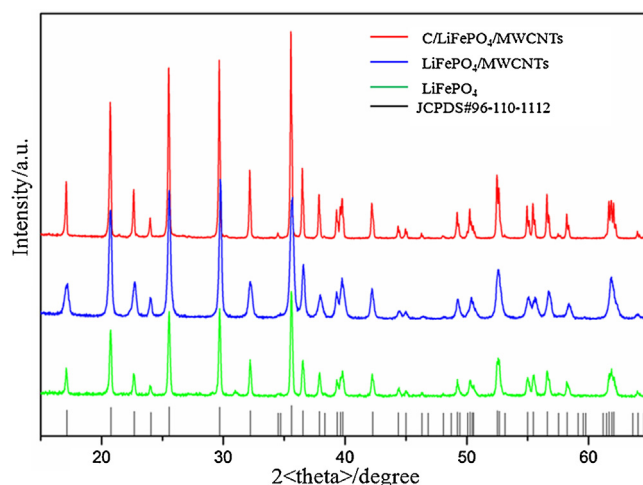


**Fig. 3.** XRD patterns for all LiFePO$_4$ samples.

solution in ethylene carbonate, diethyl carbonate and dimethyl carbonate (1:1:1, in volume) as the electrolyte. The electrode performance was investigated in terms of Cyclic voltammetry curve, charge/discharge curves and cycling capacity using a NEWARE battery-testing system (Neware Co., Ltd., China) at the cut-off voltages of 2.5 and 4.2 V. Electrochemical impedance spectroscopy (EIS) was measured using CHI604D (CH Instruments, China). EIS measurements were carried out in the frequency range from 1 mHz to 1 MHz with an AC voltage signal of ±5 mV. All the electrochemical measurements were carried out at room temperature, and the potentials were given with respect to Li$^+$/Li.

## 3. Results and Discussion

### 3.1. Structure and morphology

XRD was used to detect the crystallinity information of the as prepared pristine LiFePO$_4$,LiFePO$_4$/MWCNTs and C/LiFePO$_4$/MWCNTs submicro sized particles (Fig. 3), trivalent iron as a cheap starting material was reduced to the divalent one at this stage as confirmed by X-ray photoelectron spectroscopy, all intense peaks in the spectrum can be well indexed to orthorhombic LiFePO$_4$ (JCPDS Card No. 96 − 110 − 1112) [25]. Calculation of the pattern gave the lattice parameter values of a =5.9438 Å, b =10.3043 Å, c= 4.6857 Å and a unit cell volume of 286.95 Å$^3$, which were in good agreement with the literature values [26,27].The profiles of the reflection peaks are quite narrow, indicating the high crystallinity of the LiFePO$_4$ samples.

No obvious peaks corresponding to carbon are found in the XRD pattern possibly ascribed to its low content. However, Raman shift, evidencing the presence of carbon in the carbon-coated LiFePO$_4$ composites (Fig. 4). In Fig. 4,the strong peaks at 1342 and 1578 cm$^{-1}$ are contributed to D-band and G-band,respectively. The G-band presents for the vibration mode of graphite carbon, whereas D band stands for the disorders or defects in the graphite structure. The intensity ratio of D and G bands (I$_D$/I$_G$) represents the degree of surface disordering of coated carbon layer. The value of I$_D$/I$_G$ for LiFePO$_4$/MWCNTs and C/LiFePO$_4$/MWCNTs are 1.01 and 0.79, respectively. The higher I$_D$/I$_G$ ratio implies more defects of the LiFePO$_4$/MWCNTs samples, demonstrating that the presence of MWCNTs helps to create ordered carbon and the load of uniform-thickness PANI carbon layer further improves the disorder of C/LiFePO$_4$/MWCNTs to some extent.

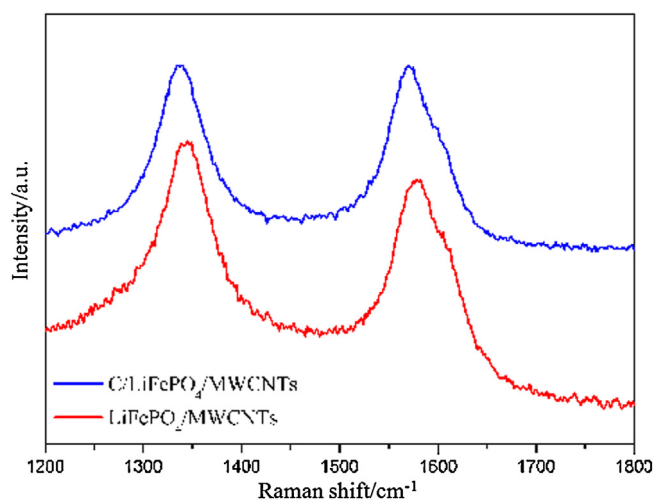The carbon contents of modified products were measured by using elemental analysis and they were found to be

**Fig. 4.** Raman spectra of LiFePO$_4$/MWCNTs and C/LiFePO$_4$/MWCNTs.

2.6%,4.2wt%,respectively, for LiFePO$_4$/MWCNTs composite, and C/LiFePO$_4$/MWCNTs sample. The low carbon content is beneficial to increasing its tap density and makes it more promising in industrial production and application. The tap density of the prepared C/LiFePO$_4$/MWCNTs material and LiFePO$_4$/MWCNT reach 2.25 g cm$^{-3}$ and 2.31 g cm$^{-3}$,respectively, which was slightly lower than that of the pure LiFePO$_4$ composite (2.80 g cm$^{-3}$) because of the addition of carbon. The higher tap density of cathode material pronouncedly makes a significantly higher volumetric energy density. It is pointed out that the nitrogen content for C/LiFePO$_4$/MWCNTs sample was detected by 0.01% implying that there is little trace of nitrogen retention and it contributes negligible influence to the final sample. In addition, the interconnected three-dimensional networks and the overall carbon coating are good for the electrical conductivity of the C/LiFePO$_4$/MWCNTs particles.

The electrical conductivity of the C/LiFePO$_4$/MWCNTs material measured by a four-point probe method was 2.1 ×10$^{-1}$ S cm$^{-1}$, which was 5.6 times higher than that for pristine LiFePO$_4$ (3.7 × 10$^{-2}$ S cm$^{-1}$) and 3.2 times higher than that of the LiFePO$_4$/MWCNTs (6.5 × 10$^{-2}$ S cm$^{-1}$), clearly showing that the electrical conductivity of C/LiFePO$_4$/MWCNTs submicro sized particles have been remarkably enhanced by the incorporation of interwaved network and the uniform load of PANI.

SEM micrographs Fig. 5 (a), (b) and (c) shows that the pristine without MWCNTs modified LiFePO$_4$ particles are several submicrons in size and highly porous. Fig. 5d reveals a porous structure of C/LiFePO$_4$/MWCNTs was formed during the final calcination process. Fig. 5(d), (e) and (f) display that the cross-linked, interlaced carbon nanotube networks are intimately embedded and incorporated into the porous LiFePO$_4$ particle structure. The LiFePO$_4$ particles in the sample is in the pattern of numerous sub-micro sized apertures, well-proportioned and narrowly distributed around 0.5 μm,constructing a 3D interconnected pore system, these small apertures lead into much larger voids inside the particles, indicating the interior pore system is interlaced. Fig. 5(g) shows the C/LiFePO$_4$/MWCNTs sample was prepared without any impurities. Fig. 5(h) implied that the single-crystalline nature of C/LiFePO$_4$/MWCNTs.

High-resolution TEM image of the LiFePO$_4$ particles in Fig. 5(i), confirms a thin carbon layer with a thickness in the range of 1–3 nm was coated into the LiFePO$_4$ particles, which was classified to be effective in achieving optimized rate capabilities. The incorporation of MWCNTs and the complete carbon coating around or between the particles which greatly enhance the surface area, favouring the

diffusion kinetics of lithium ions, are expected to contribute to the improved electrochemical properties of the composites.

### 3.2. Electrochemical Performance of LiFePO$_4$ composites

Cyclic voltammetry was conducted in order to investigate the effect of the electrochemical properties of the LiFePO$_4$ samples by using a scanning rate of 0.1mVs$^{-1}$ to 2mVs$^{-1}$, voltage range: 2.4–4.2 V. A single pair of sharp oxidation and reduction peaks, ascribing to the two-phase reaction of the Fe$^{3+}$/Fe$^{2+}$ redox couple (i.e., lithium insertion and extraction), can be clearly discerned[28]. Fig. 6(a) compared the CV profiles of pristine LiFePO$_4$,LiFePO$_4$/MWCNTs and C/LiFePO$_4$/MWCNTs in the first cycle. For pristine LiFePO$_4$, the oxidation and reduction peaks occur at 3.64 and 3.24 V, respectively, with the polarization being 0.4 V. For LiFePO$_4$/MWCNTs, the oxidation and reduction peaks are located at 3.60 and 3.30 V, respectively, and the polarization is 0.3 V. For C/LiFePO$_4$/MWCNTs,the oxidation and reduction peaks appears at 3.55 and 3.35 V, respectively, with the polarization covers 0.2 V. Broadened peaks of pristine LiFePO$_4$ present the most poor kinetics, lithium intercalation and deintercalation is sluggish. The lower polarization and higher peak of C/LiFePO$_4$/MWCNTs sample compared with that of LiFePO$_4$/MWCNTs can be attributed to the higher electronic conductivity further improved by PANI carbon layer coating [29].

Fig. 6(b) and (c) shows the cyclic voltammetry curves of LiFePO$_4$/MWCNTs and C/LiFePO$_4$/MWCNTs at an increasing scan rate from 0.5 to 2 mV s$^{-1}$, respectively. The cathodic (I$_{pc}$) and anodic (I$_{pa}$) peak currents versus the square root of the scan rate was presented in order to obtain the apparent anodic and cathodic diffusion constants for both LiFePO$_4$ samples, n$^{1/2}$, in the 0.2–1 mV s$^{-1}$ range (Fig. 6(d)). The diffusion constants for the Li$^+$ ions in the samples were calculated according to the Randles-Sevcik equation[30,31], I$_p$/m = 0.4463F(F/RT)$^{1/2}$A$_e$(D$_{app}$)$^{1/2}$C$_{Li}$*v$^{1/2}$.I$_p$ presents for the peak current, m is the mass of the electrode, F stands for Faraday constant, where A$_e$ is the effective area of the electrode per unit mass. It should be point out that LiFePO$_4$ has a one-dimensional diffusion path in the [010] plane, and A$_e$ thus is denoted one-third of the total BET surface area of LiFePO$_4$, which is 5.45 m$^2$ g$^{-1}$ for LiFePO$_4$/MWCNTs and 6.68 m$^2$ g$^{-1}$ for C/LiFePO$_4$/MWCNTs.

Where D$_{app}$ is the apparent diffusion constant for Li$^+$ ions, C$_{Li}$* is the Li$^+$ concentration in a particle before delithiation, and v is the CV scan rate. Considering the parameters of A (electrode area), C (concentration of Lit) and n (number of electrons involved in the redox process) are constants for both electrodes, the diffusion coefficient of lithium (D$_{Li}$) of C/LiFePO$_4$/MWCNTs is found to be 1.18 times higher than that of LFP/MWCNTs. The linear dependence of peak current (I$_p$) of CV of samples on the square root of scan rate (v$^{1/2}$)can be observed Fig. 6,which can also be concluded from the comparison Fig. 6(b) with Fig. 6(c). Therefore, the coating of carbon layer originated from PANI in C/LiFePO$_4$/MWCNTs is uniform and it further improves transportation of Li ions during cell operation compared to LiFePO$_4$/MWCNTs. These results indicate that the lithium diffusion constant for the C/LiFePO$_4$/MWCNTs electrode was enhanced by uniform submicro sized particles, the hierarchical porous structure,3D networks, and the overall carbon coating.

Fig. 7(a,b,c) displays the galvanostatic charge discharge voltage profiles of cells for all LiFePO$_4$ samples at progressively increasing C rates from 0.1 C to 5 C between 2.2 and 4.2 V vs. Li$^+$/Li. Accordingly, the dependence of specific capacity on current density was shown in Fig. 7(d). It is noted the voltage plateau is lengthened for the MWCNTs modified LiFePO$_4$ materials, which should be attributed to the higher electrochemical reactivity of modified LiFePO$_4$ and excellent kinetics. This result is in accordance with the CV profiles. The modified LiFePO$_4$ materials exhibit higher capacities than pure LiFePO$_4$ at a low rate C/10, and a maximum capacity of
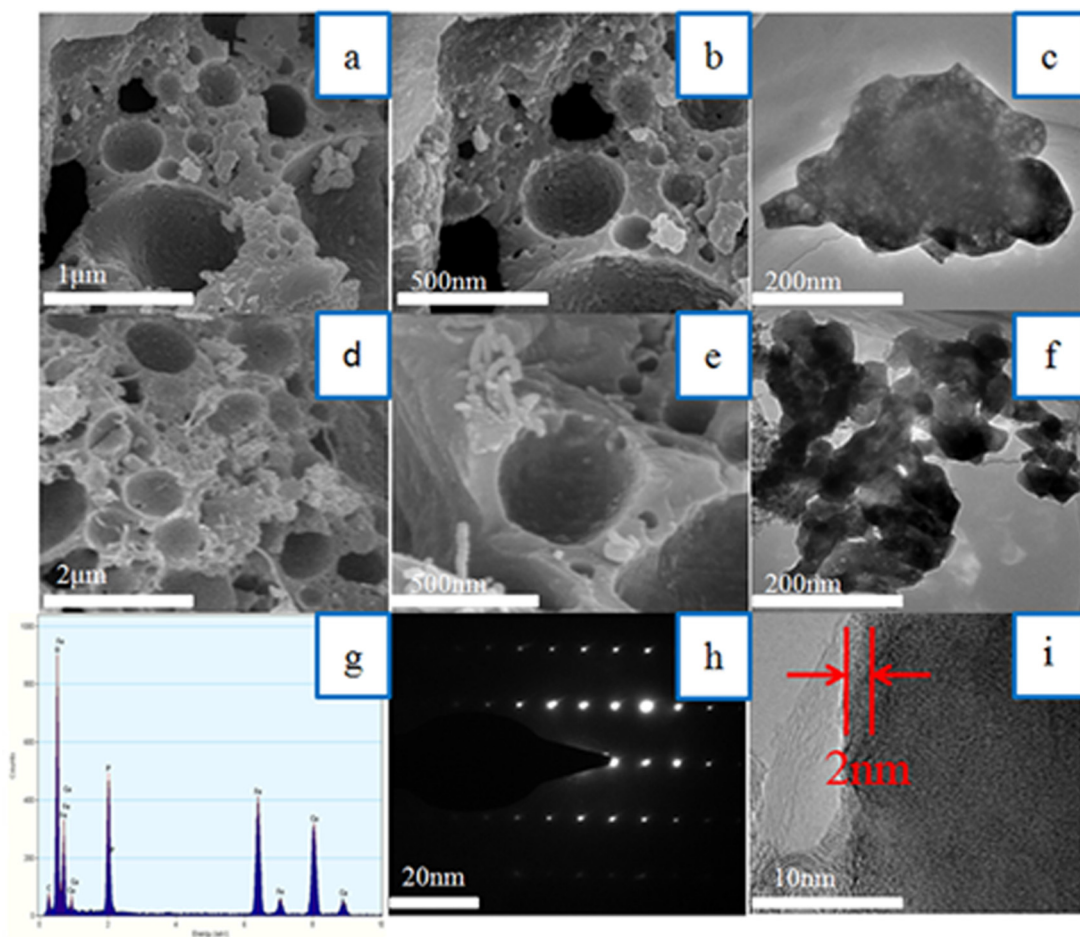
**Fig. 5.** (a),(b)SEM image at various magnifications,(c)TEM image for pure LiFePO$_4$;(d),(e)SEM image at various magnifications, (f) TEM image, (g) element mapping, (h) elected area electron diffraction (SAED) pattern, (i) HRTEM image for C/LiFePO$_4$/MWCNT sample.

169.6mAhg$^{-1}$ (nearly to its theoretical capacity 170mAhg$^{-1}$) are found in C/LiFePO$_4$/MWCNTs, while that of the MWCNTs/LiFePO$_4$ and pure LiFePO$_4$ reach 158.9, 137.2 mAhg$^{-1}$,respectively.Bare LiFePO$_4$ displays lower capacity than modified LiFePO$_4$ samples because of the lower lithium diffusion constant and electronic conductivity. Meanwhile, it presents a serious polarization tendency at high C rates, while the modified samples have a slight polarization tendency.

The cycle performances of modified samples were extensively explored from 0.1 C to 20 C in Fig. 8(a). As shown in Fig. 8(a), the LiFePO$_4$/MWCNTs and C/LiFePO$_4$/MWCNTs samples have a stable cycle performance at these rates. C/LiFePO$_4$/MWCNTs exhibited a good rate performance with a capacity of 141.9 mAh g$^{-1}$ at a relatively high rate of 20 C, whereas that for LiFePO$_4$/MWCNTs was just 83.9 mAh g$^{-1}$. When the current density reverts back to a low current density of C/10 rate, the specific capacities of the electrode materials were able to recover to the original discharge capacity, displaying its good reversibility, which is a highly desirable property for electrode materials in lithium ion batteries. These results depicted that the decreased submicro sized particles, tridimensional networks and full carbon coatings in hierarchical porous structure throughout the modified LiFePO$_4$ powder ensure transfer electrons through all directions and alleviate the polarization. The capacity fading could be ascribed to the slow diffusion of lithium-ion in LiFePO$_4$ and the poor contact between the LiFePO$_4$ particles and conductors.

To evaluate the effect of this submicroarchitecture on fast electrochemical reaction kinetics, the submicroforest cathodes under investigation were subjected to a rather abusive high rate testing protocol in which the cells were both charged and discharged at the higher rates. The carbon coating further improved the morphology and structural stability of 3D LiFePO$_4$ submicroforest cathode. As depicted in Fig. 8(b), the submicrosized C/LiFePO$_4$/MWCNTs particles still delivered discharge capacity of 153.7 mAh g$^{-1}$ at the 10 C rate after 200 cycles, corresponding to 99.1% of the capacity retention, 141.9 mAh g$^{-1}$ at 20 C with 98.3% the capacity retention, implying that the structural robustness of the well-crystallized hierarchical porous LiFePO$_4$ submicrosized particles. Discharge capacity remained virtually unchanged after 200 cycles, indicating highly reversible lithium insertion/extraction kinetics. The C/LiFePO$_4$/MWCNTs cathode material with outstanding stability supplies a platform to realize high power applications in lithium ion batteries.

Electrochemical impedance spectroscopy (EIS) examination of the coin cells was conducted to further clarify the difference in the electrochemical response of three LiFePO$_4$ cathode materials. As depicted in Fig. 9(a),these impedance spectra combined of a depressed semicircle in the high frequency region and a straight line in the low-frequency region, and a simple equivalent circuit was established to simulate the spectra (the inset in Fig. 9(a)). The semicircle is mainly associated to the charge-transfer resistance and the corresponding capacitances at the electrode/electrolyte interface, the straight line in the low frequency region is related with the diffusion behavior of lithium ions within the LiFePO$_4$ particles [32,33].

The intersection with the real axis at high frequency corresponds to ohmic resistance Rohm reflects the electronic and
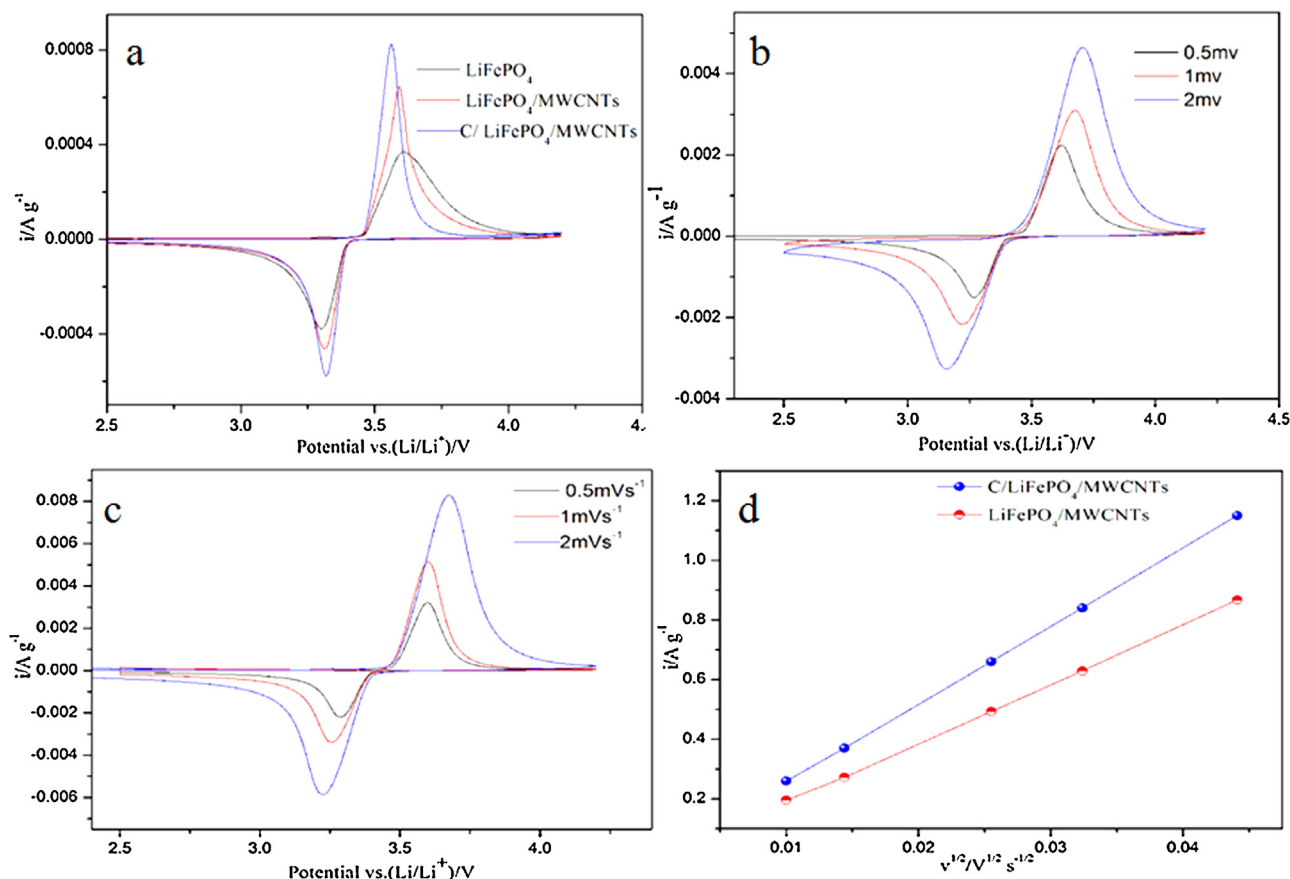
**Fig. 6.** A Cyclic voltammetry curves of all LiFePO4 samples at C/10 rate,(b) cyclic voltammetry curves for LiFePO4/MWCNTs, and (c) C/LiFePO4/MWCNTs samples at various scan rates,(d) The relationship of peak current ($i_p$) and the square root of scan rate ($n^{1/2}$) for both samples.

ionic resistance of the two electrodes and electrolyte/separator. Considering the resistance of electrolyte/separator can be assumed to the same, the smaller Rohm Since the faradaic reaction is determined by electron conduction and ion transfer, the reduction of resistance might be attributed to the enhancement of the electronic conductivity of the C/LiFePO4/MWCNTs electrodes arising from the co-modication of the hierarchical porous carbon structure and the carbon-coated layers, which could allow better penetration of electrolyte, achieve a higher surface area and reduce the charge transfer resistance. The charge-transfer resistance was calculated from the semicircle in the high-middle frequency range as about 130 Ω, 80 Ω and 40 Ω for the pristine LiFePO4,LiFePO4/MWCNTs and C/LiFePO4/MWCNTs, respectively, the C/LiFePO4/MWCNTs electrode exhibits lower charge-transfer resistance, suggesting that their electrolyte–electrode complex reactions can take place easily. The bigger slope of impedance of modified LiFePO4 samples indicate their higher electrochemical activity, which ascribed to hierarchical porous structure facilitate the diffusion path of lithium ion. The improved lithium-ion diffusion process within C/LiFePO4/MWCNTs particles estimated from the oblique line at low frequencies is greatly enhanced by tridimensional networks allowing uniform carbon coating and electrolyte penetration, improving the electronic conductivity and reducing the diffusion path of the lithium ions. Those results are in agreement with the CV profiles, rate performance and cycling behavior results.

Fig. 9(b) shows the relationship between $Z_{Re}$ and square root of frequency ($w^{-1/2}$) in the low frequency region. With Eq. (2), it is obtained that the Warburg impedance coefficient ($\sigma w$) of the LiFePO4 samples increase with the additive of MWCNTs and further rise when modified by PANI carbon layer, which

are 6.85, 11.19,18.36 cm$^2$ s$^{-1/2}$, respectively for pure LiFePO4, LiFePO4/MWCNTs and C/LiFePO4/MWCNTs.

$$Z_{Re} = Re + Rct + \sigma_w\omega^{-1/2} \tag{1}$$

$$D = R^2T^2/2A^2n^4F^4C^2\sigma_W^2 \tag{2}$$

Based on the obtained Warburg impedance coefficients, the Li-ion diffusion coefficients of samples can be calculated using Eq. (2),where D is Li-ion diffusion coefficient (cm$^2$ s$^{-1}$), R is gas constant (8.314 J mol$^{-1}$ K$^{-1}$), T is the absolute temperature (K), A is the electrode area (cm$^2$), n is the number of electrons involved in the redox process (1 in our case), C is the shuttle concentration (7.69 × 10$^{-3}$ mol cm$^{-3}$) and F is the Faraday constant (96486 C mol$^{-1}$).The Li-ion diffusion coefficients of the LiFePO4 samples for pure LiFePO4, LiFePO4/MWCNTs and C/LiFePO4/MWCNTs are extracted to be 1.38 × 10$^{-12}$,4.57 × 10$^{-12}$,1.24 × 10$^{-11}$,respectively.The result clearly manifests that the Li-ion diffusion coefficient of LiFePO4 nanocomposites initially increases with increase of the modification of MWCNTs conductive network which would increase the conductive interconnection among the adjacent LiFePO4 particles, and then are enhanced with further load of the PANI carbon layer which forms more conductive paths for electrons improve the electrons transfer efficiency and benefit the electrical conductivity of LiFePO4. It is consistent with the conclusion presented above that the carbon coating can increase both the ionic and electronic conductivity of the LiFePO4 nanocomposites. Besides, the porous structure formed in the network structure provides diffusion path and facilitates the diffusion of lithium ions at high rate charge and discharge. The BET surface area of porous C/LiFePO4/MWCNT is as high as 20 m$^2$ g$^{-1}$which is much higher
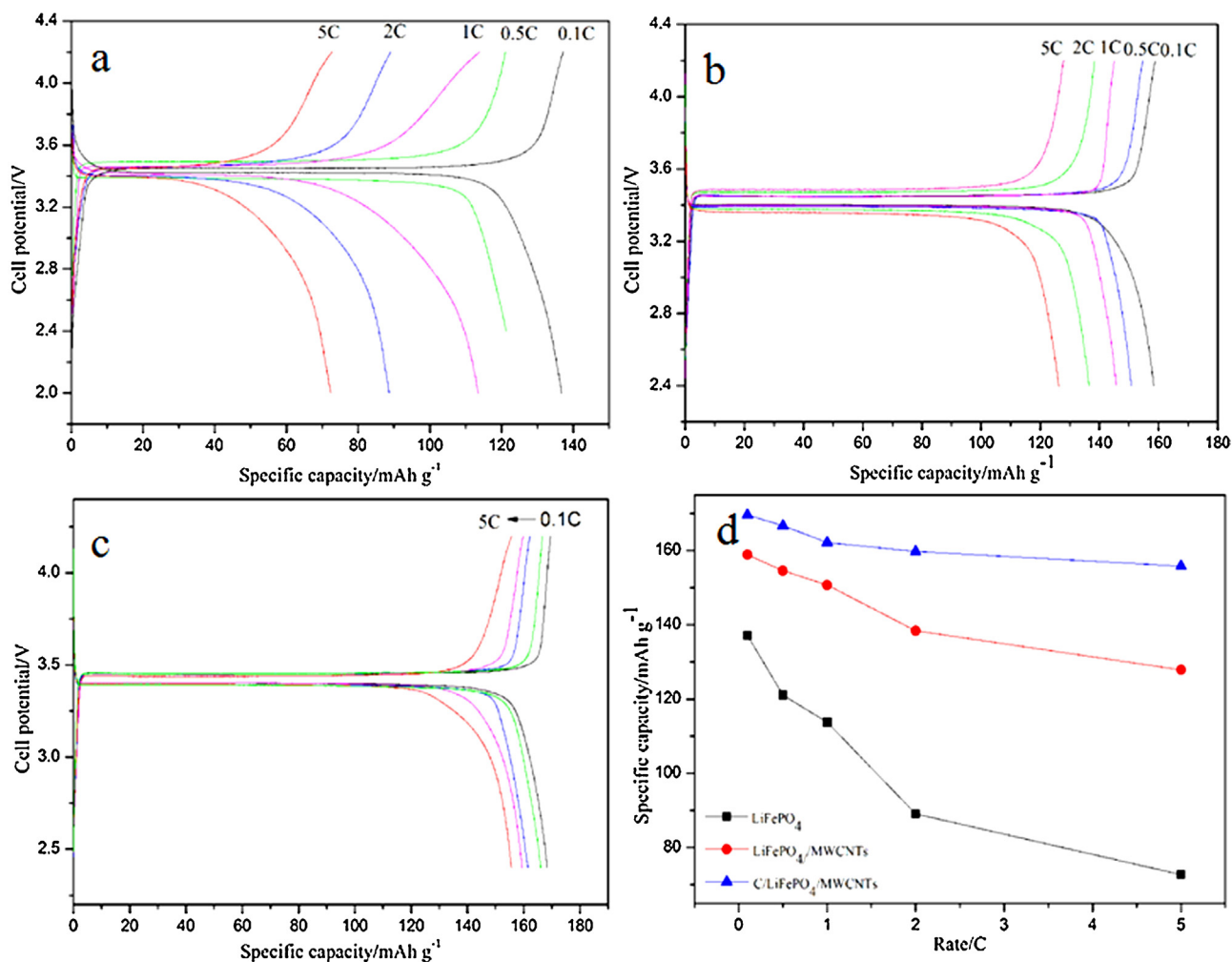
**Fig. 7.** Charge/discharge curves of (a) pristine LiFePO$_4$ sample,(b) LiFePO$_4$/MWCNTs composite,(c) C/LiFePO$_4$/MWCNT sample at different current densities, and (d) the dependence of specific capacity on current density.

than that of LiFePO$_4$/MWCNTs 15 m$^2$ g$^{-1}$ and that of pristine LiFePO$_4$ sample 9m$^2$ g$^{-1}$, which increases the interfacial contact between LiFePO$_4$ particles and the surrounding electrolyte solution.

Excellent electrochemical discharge rates can be achieved with LiFePO$_4$ nanoplates. Their power and energy performances were further evaluated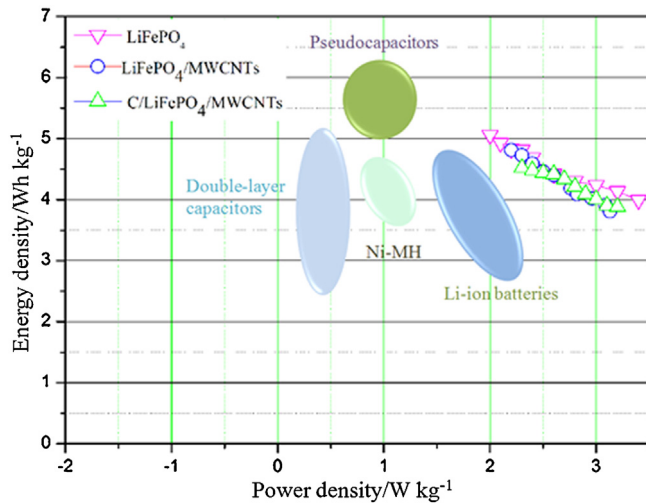 with a Ragone plot, compared with some advanced energy storage and conversion devices (Fig. 10).At a low specific power of < 1 kW kg$^{-1}$, C/LiFePO$_4$/MWCNT exhibits power density as high as 16.8 kW kg$^{-1}$(energy density: 84 Wh kg$^{-1}$), indicating high energy-storage performances. In the case of LiFePO$_4$/MWCNT, an ultrahigh power density of 14 kW kg$^{-1}$(energy density:70Wh kg$^{-1}$) can be realized, while pure LiFePO$_4$ can afford 12 kW kg$^{-1}$(energy density:60 Wh kg$^{-1}$).
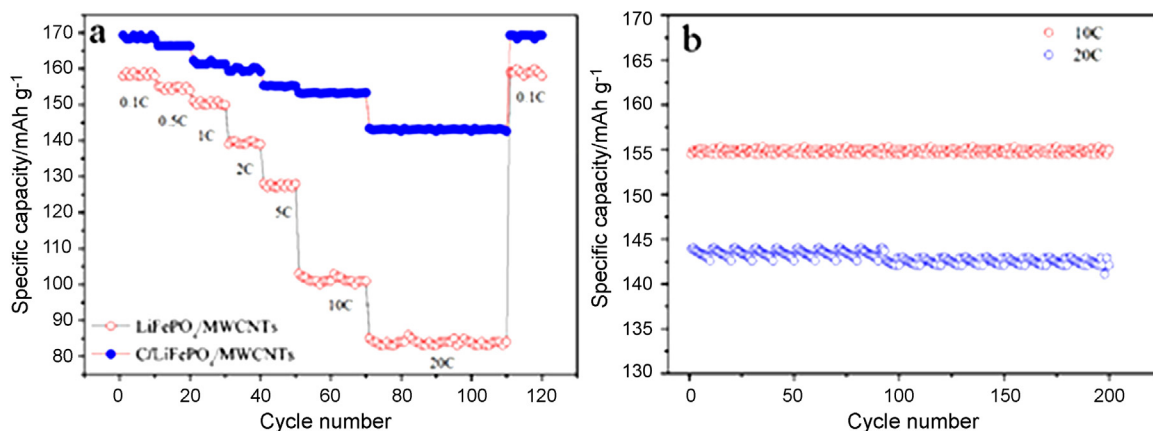


**Fig. 8.** The rate performance curves of (a) MWCNTs modified LiFePO$_4$ materials at various current rates, (b) long-term stability for C/LiFePO$_4$/MWCNTs material at high current rates.
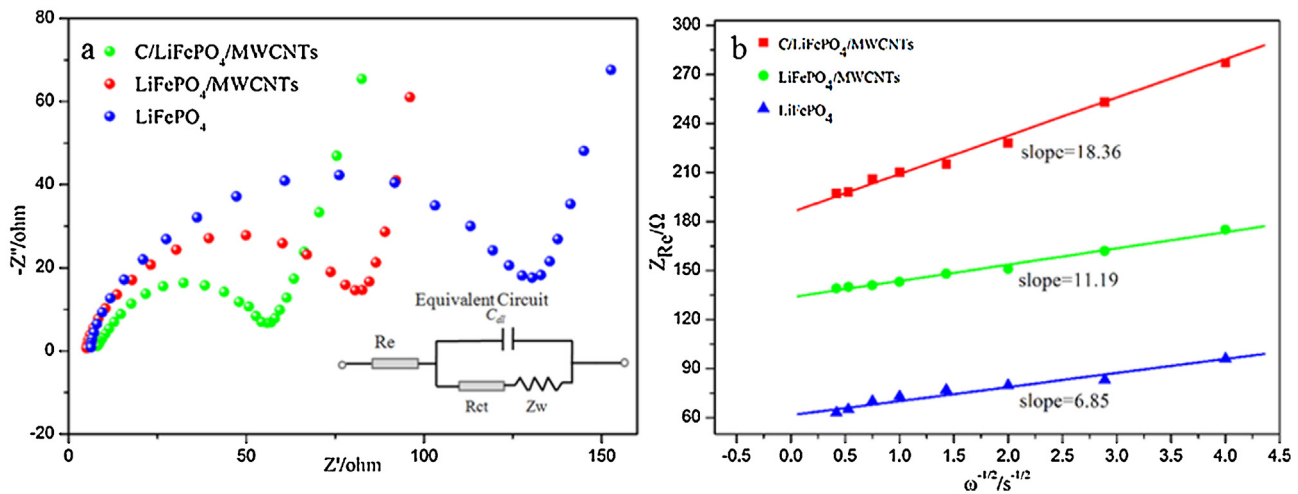
**Fig. 9.** a Electrochemical impedance spectroscopy (EIS) result of the LiFePO$_4$ samples, the inset of (a) shows an equivalent circuit. (b) The relationship between $Z_{Re}$ and $\omega^{-1/2}$ at low frequency.



**Fig. 10.** The Ragone plot of the LiFePO$_4$ samples, in comparison with some advanced energy storage and conversion devices.

The energy densities and corresponding power densities were calculated from the following equations [34], and the result at 30A g$^{-1}$ is listed in Table 1:

$$P = \frac{V^2}{4RM} \quad (3)$$

$$E = \frac{1}{2}CU^2 = \frac{1}{8}MC_{SP}V^2 \quad (4)$$

where V is the applied voltage, R is the equivalent series resistance (ESR), M is the total mass of the electrodes, and C is the total capacitance of electrode (C = C$_{SP}$M/4).

Such cells could supply higher power densities than current nickel metal-hydride (100-1000 W kg$^{-1}$) and general lithium-ion

battery (800-2000 W kg$^{-1}$), while the energy densities are several times of that of supercapacitor technology (1-20Wh kg$^{-1}$). These capabilities indicate that such C/LiFePO$_4$/MWCNT cathode material can be used to build superior energy storage and conversion devices (e.g., HEVs, and EVs) with both high-power and high-energy densities.

As discussed above, such an attractive high performance of C/LiFePO$_4$/MWCNTs can be ascribed to well mixed conducting materials, interconnected tridimensional submicro-networks, hierarchical porous structure, and well crystallization advantage. The effective dispersion of hierarchical structure and uniform carbon layer not only allow better penetration of electrolyte to promote lithium ion diffusion but also increase the electrochemical reaction surface, thus ultimately alleviate electrode polarization, simultaneously, provide a good stability and capacity retention. The well crystallized and submicro particles present a high tap density, in turn, develop a high rate capability.

## 4. Conclusions

In conclusion, hierarchically structured composites based on porous LiFePO$_4$ with MWCNTs networks present significantly improved specific capacity and rate performance in comparison to unmodified LiFePO$_4$ when used in lithium ion batteries. The prepared C/LiFePO$_4$/MWCNTs composites present an excellent rate capability and capacity retention. The improved electrochemical performance of the carbon-coated composites could be attributed to the combined effects of the hybrid structure, the carbon layers on particles, and the porous particles embedded in the carbon matrix, which enhance the structural stability and improve the lithium storage kinetics by facilitate the transport path of electrons and ions, therefore presents an intriguing route to design enhanced electrode structures for a wide variety of applications in electrochemical energy storage and conversion.

**Table 1**
Power Density, And Energy Density of LFP Electrodes at current density 30 Ag$^{-1}$ (20C).

| Samples | Power density (kW kg$^{-1}$) | Energy density (Wh kg$^{-1}$) |
|---------|------------------------------|-------------------------------|
| LFP | 12 | 60 |
| LFP/MWCNT | 14 | 70 |
| C/LFP/MWCNT | 16.8 | 84 |

## References

[1] A. Yamada, S.C. Chung, K. Hinokuma, Optimized LiFePO$_4$ for lithium battery cathodes, Journal of Electrochemical Society 148 (2001) 224.

[2] P.P. Prosini, M. Carewska, S. Scaccia, P. Wisniewski, M. Pasquali, Long-term cyclability of nanostructured LiFePO$_4$, Electrochimica Acta 48 (2003) 4205.

[3] L. Kavan, I. Exnar, J. Cech, M. Graetzel, Mesoporous silica materials with covalently anchored phenoxazinone dyes as fluorescent hybrid materials for vapour sensing, Journal of materials chemistry 19 (2007) 4716.

[4] C.M. Doherty, R.A. Caruso, B.M. Smarsly, C.J. Drummond, Hierarchically porous monolithic LiFePO$_4$/carbon composite electrode materials for high power lithium ion batteries, Journal of materials chemistry 21 (2009) 5300.

[5] J. Liu, F.K. Liu, G.L. Yang, X.F. Zhang, J.W. Wang, R.S. Wang, The preparation of conductive nano-LiFePO$_4$/PAS and its electrochemical performance, Electrochimica Acta 55 (2010) 1067.

[6] K. Kim, J.-H. Jeong, I.-J. Kim, H.-S. Kim, Carbon coatings with olivine oil, soybean oil and butter on nano-LiFePO$_4$, Journal of power Sources 167 (2007) 524.

[7] K.S. Park, S.B. Schougaard, J.B. Goodenough, Conducting-Polymer/Iron-Redox-Couple Composite Cathodes for Lithium Secondary Batteries, Advanced Materials 19 (2007) 848.

[8] K. Wang, R. Cai, T. Yuan, X. Yu, R. Ran, Z.P. Shao, progress investigation, electrochemical characterization and optimization of LiFePO$_4$/C composite from mechanical activation using surcrose as carbon source, Electrochimica Acta 54 (2009) 2861.

[9] P. Subramany Herle, B. Ellis, N. Coombs, L.F. Nazar, Nano-network electronic conduction in iron and nickel olivine phosphates, Nature Materials 3 (2004) 147.

[10] K.S. Park, J.T. Son, H.T. Chung, S.J. Kim, C.H. Lee, K.T. Kang, H.G. Kim, Surface modification by silver coating for improving electrochemical properties of LiFePO$_4$, Solid State Communications 129 (2004) 311.

[11] J.B. Heo, S.B. Lee, S.H. Cho, J. Kim, S.H. Park, Y.S. Lee, Synthesis and electrochemical performance of LiFePO$_4$/grapheme composites by solid–state reation, Materials Letters 63 (2009) 581.

[12] E.M. Jin, B. Jin, D.-K. Jun, K.-H. Park, H.-B. Gu, K.-W. Kim, A study on the electrochemical characteristics of LiFePO$_4$ cathode for lithium polymer batteries by hydrothermal method, Journal of power Sources 178 (2008) 801.

[13] Q. Wang, S.M. Zakeeruddin, D. Wang, I. Exnar, M. Grätzel, Redo Targeting of Insulating Electrode Materials: A New Approach to High-Energy-Density Batteries, Angewandte Chemie International Edition 45 (2006) 8197.

[14] R. Dominko, M. Bele, J.M. Goupil, M. Gaberscek, M. Remskar, D. Hanzel, I. Arcon, J. Jamnik, Wired porous cathode materials:a novel concept for synthesis of LiFePO$_4$, Chemical Materials 19 (2007) 2960.

[15] Y.S. Hu, P. Adelhelm, B.M. Smarsly, S. Hore, M. Antonietti, J. Maier, Synthesis of Hierarchically Porous Carbon Monoliths with Highly Ordered Microstructure and Their Application in Rechargeable Lithium Batteries with High-Rate Capability, Adanced Functional Materials 17 (2007) 1873.

[16] X.L. Wu, L.Y. Jiang, F.F. Cao, Y.G. Guo, L.J. Wan, LiFePO$_4$ Nanoparticles Embedded in a Nanoporous Carbon Matrix: Superior Cathode Material for Electrochemical Energy-Storage Devices, Advanced materials 21 (2009) 2710.

[17] G. Wang, Q. Zhang, Z. Yu, M. Qu, The effect of different kinds of nano-carbon conductive additives in lithiumion batteries on the resistance and electrochemical behavior of theLiCoO$_2$ composite cathodes, Solid State Ionics 179 (2008) 263.

[18] X.L. Li, F.Y. Kang, X.D. Bai, W. Shen, A novel network cathode composite cathode of LiFePO$_4$/multiwalled carbonnanotubes with high capability for lithium batteries, Elecrochemical Communications 9 (2007) 663.

[19] L. Wang, Y.D. Huang, R.R. Jiang, D.Z. Jia, Nano-LiFePO$_4$/MWCNT Cathode Materials Prepared by Room-Temperature Solid-State Reaction and Microwave Heating, Journal Electrochemical Society 154 (2007) A1015.

[20] T. Muraliganth, A.V. Murugan, A. Manthiram, Nanoscale networking of LiFePO$_4$ nanorods synthesized by a microwave-solvothermal route with carbon nanotubes for lithium ion batteries, Journal of Materials Chemistry 18 (2008) 5661.

[21] J.L. Yang, J.J. Wang, X.F. Li, D.N. Wang, J. Liu, G.X. Liang, M. Gauthier, Y.L. Li, D.S. Geng, R.Y. Li, X.L. Sun, Hierarchically porous LiFePO$_4$/nitrogen-doped carbon nanotubes composite as a cathode for lithium ion batteries, Journal of materials chemistry 22 (2012) 7537.

[22] Y. Zhou, J. Wang, Y. Hu, R. O'Hayreb, Z. Shao, A porous LiFePO$_4$ and carbon nanotube composite, Chemical Communications 46 (2010) 7151.

[23] Y.Y. Liu, C.B. Cao, J. Li, Enhanced electrochemical performance of car-bonnanospheres -LiFePO$_4$ composite by PEG based sol-gel synthesis, Electrochimica Acta 55 (2010) 3921.

[24] Q. Zhang, Z. Chang, M. Zhu, X. Mo, D. Chen, Electrospun carbon nanotube composite nanofibres with uniaxially aligned arrays, Nanotechnology 18 (2007) 115611.

[25] V.A. Streltsov, E.L. Belokoneva, V.G. Tsirelson, N.K. Hansen, Multipole analysis of the electro density in triphylite,LiFePO$_4$,using X-ray diffraction data, Acta Crystallographica Section B 49 (1993) 147.

[26] X. Wu, L. Jiang, F. Cao, Y. Guo, L. Wan, LiFePO4 Nanoparticles Embedded in a Nanoporous Carbon Matrix: Superior Cathode Material for Electrochemical Energy-Storage Devices, Advanced Materials 21 (2009) 2710.

[27] J. Zheng, X. Li, Z. Wang, H. Guo, S. Zhou, LiFePO$_4$ with enhanced performance synthesized by a novel synthetic route, Journal of Power Sources 184 (2008) 574.

[28] J. Yao, F. Wu, X. Qiu, N. Li, Y. Su, Effect of CeO$_2$-coating on the electrochemical performances of LiFePO$_4$/C cathode material, Electrochimica Acta 56 (2011) 5587.

[29] J.K. Kim, J.Q. Choi, G.S. Chauhan, J.H. Ahn, G.C. Hwang, J.B. Choi, H.J. Ahn, Enhanced of electrochemical performance of lithium iron phosphate by controlled sol-gel synthesis, Electrochima Acta 53 (2008) 8258.

[30] D.Y.W. Yu, C. Fietzek, W. Weydanz, K. Donoue, T. Inoue, H. Kurokawa, S. Fujitani, Study of LiFePO$_4$ by Cyclic Voltammetry, Journal of Electrochemical society 154 (2007) A253.

[31] M.Y. Cho, K.B. Kim, J.W. Lee, H. Kim, H. Kim, K. Kang, K.C. Roh, Defect-free solvothermally assisted synthesis of microspherical mesoporous LiFePO$_4$/C, RSC Advances 3 (2013) 3421.

[32] J.Y. Xiang, J.P. Tu, L. Zhang, X.L. Wang, Y. Zhou, Y.Q. Qiao, Y. Lu, Improved electrochemical performances of 9LiFePO$_4$·Li$_3$V$_2$(PO$_4$)/C composite prepared by a simple solid-state method, Journal of Power Sources 195 (2010) 8331.

[33] T. Muraliganth, A. Murugan, A. Manthiram, Nanoscale networking of LiFePO$_4$ nanorods synthesized by a microwave-solvothermal route with carbon nanotubes for lithium ion batteries, Journal of Materials Chemistry 18 (2008) 5661.

[34] Z. Chen, Y.C. Qin, D. Weng, Q.F. Xiao, Y.T. Peng, X.L. Wang, H.X. Li, F. Wei, Y.F. Lu, Design and Synthesis of Hierarchical Nanowire Composites for Electrochemical Energy Storage, Advanced Functional Materials 19 (2009) 3420.